THE STUDY OF MATERIAL PROPERTIES USING CHANNELING RADIATION

R.H. Pantell, J.O. Kephart, R.K. Klein
Stanford University
Stanford, CA 94305

H. Park
AT&T Bell Laboratories
1247 South Ceder Crest Blvd.,
Allentown, Pennsylvania 18103

B.L. Berman
211 Samson Hall
George Washington University
Washington, DC 20052

S. Datz
Oak Ridge National Laboratories
P.O. Box X
Oak Ridge, Tennessee 37830

INTRODUCTION

A possible application for channeling radiation is for investigating the properties of crystals in which the channeling occurs. In this paper we present some general considerations concerning channeling radiation as a measurement technique, and then we proceed to describe several specific examples.

I. GENERAL CONSIDERATIONS

Perhaps the first question to pose regarding any measurement procedure is whether or not the procedure alters the properties under observation. In particular, does the channeling cause a significant temperature rise in the crystal or induce a high density of defects?

Under the conditions for which we performed our measurements, the answer to both these questions is "no". Using an electron beam, the particle energy range was from 10 to 80 MeV, at an average current of $\sim 10^{-13}$ A over an area of 0.2 cm^2, with an exposure time of $\sim$ 30 minutes for a channeling radiation spectrum In a 20μ thick Si crystal, for example, the temperature rise, considering radiation cooling only, is less than 2×10^{-4}K, and the fraction of Si atoms displaced by the incident electron beam is about 1.5 parts in 10^{12}. These effects are negligible.

1

Table I: Some methods for studying crystal properties

Electron Microscopy	Ion Channeling	X-ray Diffraction	Channeling Radiation
High resolution photography	Location and identification of impurity atoms.	Measure bulk phenomena: atomic spacing, vibrational amplitudes	Measure bulk phenomena: crystal potentials, vibrational amplitudes.
Depth limited to ~ 1.0µ	Depth limited to ~ 1.0µ		
Uses electrons to a few MeV energy.	Uses positive ions in the energy range from a FEW KeV to a FEW MeV	information obtained from the intensity of a diffracted wave.	information obtained from radiation characteristics. Electron or positron energies range from 1.0 MeV to 10 GeV.
Material damage can be a problem		Can be performed on thick samples.	Sample thicknesses range from µ to mm
			Electrons and positrons are different probes.

There are a variety of methods for studying crystal properties, and Table I lists some of these approaches along with their features. These procedures complement each other, in that they can measure different parameters or, in the case that the same parameter is measured, a confirmation is provided. The properties measured by channeling radiation a similar to those determined by x-ray diffraction in that parameters are averaged over many lattice sites, whereas electron microscopy and ion channeling are sensitive to point defects and impurities.

At low particle energies, sub-MeV to several MeV, an electron microscope or Van de Graaff accelerator could provide the particles; below 30 MeV a single klystron linac or a microtron could be used; and a linac would be required for the higher energies. It is unlikely that a high energy machine would be constructed for channeling radiation studies, but for an existing accelerator the incremental cost is not great.

An interesting feature of channeling radiation as applied to material studies is that electrons and positrons provide different probes. The reason for this is that positrons channel between axes and planes, whereas electrons channel close to axes and planes.

In Table II, the various radiation parameters are listed, along with crystal properties related to these parameters. Our research program, thusfar, has utilized photon energy and spectral linewidth and intensity, to obtain information about the crystals. Photon energy, for some range of parameters, can be measured to better than one percent accuracy, whereas linewidth and intensity are determinable to 10-15% accuracy. however, if some crystal characteristic is altered, then the change in linewidth and intensity can be obtained within several percent.

Table II Radiation Parameters and Crystal Properties

<u>Radiation parameter</u>	<u>Crystal property</u>
Photon energy	Potential function, vibrational amplitude, electronic bonding.
Linewidth	Vibrational amplitude, multiple scattering, defect density.
Intensity	Scattering, potential function.
Time structure	
Direction	
Polarization	

Additional radiation parameters (time structure, direction, and polarization) might also be used for examining crystals. For example, our linac provides hard x-rays with about 10 psec duration, which could be applied to a study of ultrafast relaxation processes. Streak cameras, for detection purposes, are sensitive to wavelengths below one Angstrom with a time resolution of 10-20 psec.

II. MEASUREMENT OF CRYSTAL POTENTIALS

The location of the emission peaks in the channeling radiation spectra are specified by the crystalline potential function and by the parameters of the incident particle. A procedure that has been applied to the determination of crystalline potential function with undetermined coefficients, and then use a minimization of error technique to match the calculated spectra to the data. In this manner, a potential is obtained which can be checked against the portion of the data that was not used for the matching.

One example concerns the contribution of the covalent bonding electrons in diamond to the potential experienced by a channeled electron.[2,3] We usually calculate the potential assuming independent free atoms or ions in the crystal, and then summing the individual Hartree-Fock potentials. In Figure 1 the function obtained in this manner, designated as the "free atom" curve, is for electrons channeled by (111) planes in diamond. Another curve, based upon x-ray diffraction data, is also shown, and this latter curve incorporates electron bonding whereas the former does not. Eigenvalues are drawn for 30.5 MeV electrons using the x-ray data.

Figure 2 illustrates the spectra calculated from the two curves in Figure 1 for 30.5 and 54.5 MeV electrons, along with the experimental data. In both instances the x-ray diffraction potential provides a better match to the data. The broad emission peak that occurs at ~ 30 keV the upper figure and at ~ 60 keV in the lower results from the addition of $\Delta n = 1$ transitions between the eigenstates of Figure 1. Vibrational motion of the atoms is included in the analysis, both as a Debye-Waller factor and as a line-broadening mechanism. The presence of a $\Delta n = 3$ transition, the $3 \to 0$ for 30.5 MeV, is apparent in the data.
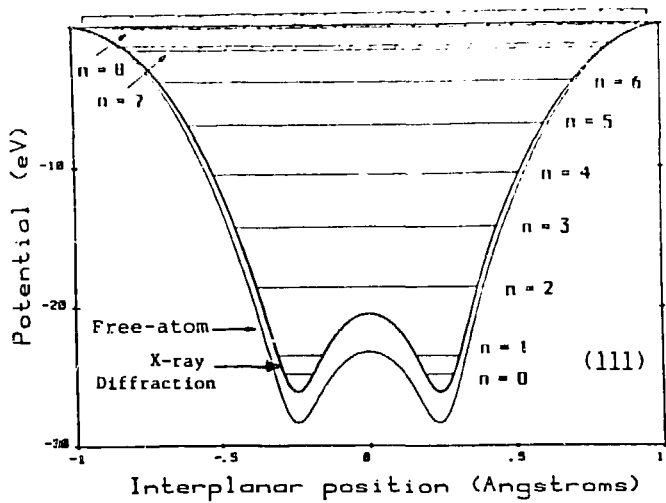
3

Figure 1: Potential functions for electrons channeling by (111) planes in diamond. X-ray diffraction data includes valence electron asymmetry, and the free-atom calculation does not.
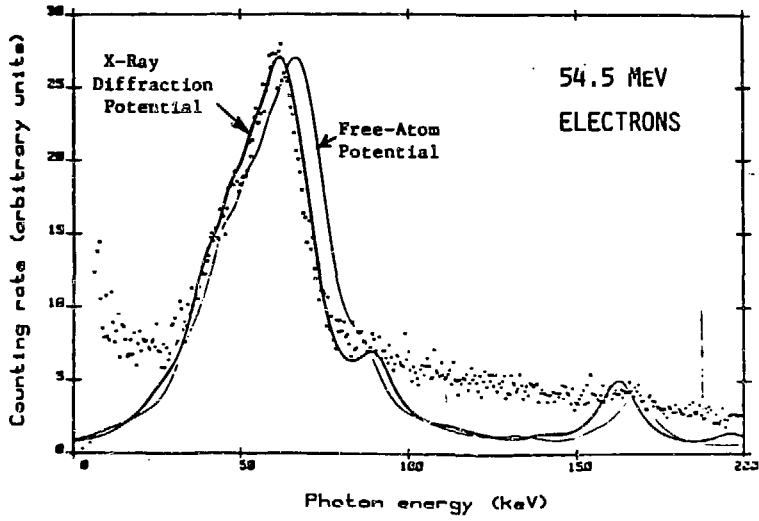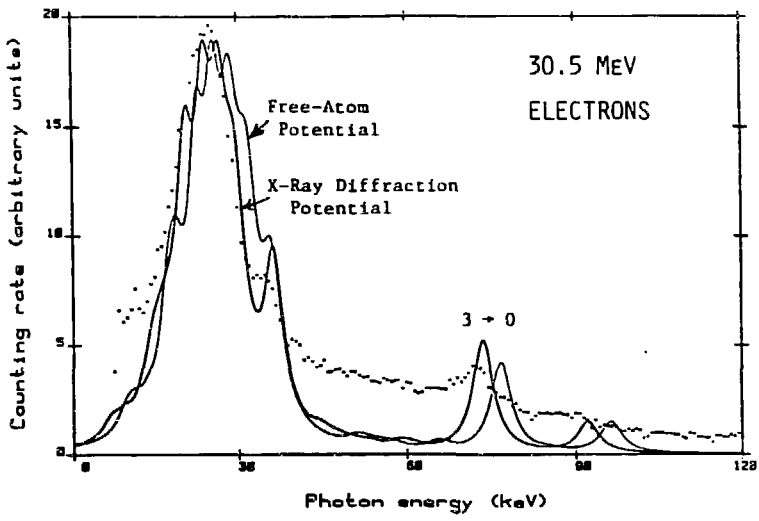

Figure 2: Calculated and Measured spectra from (111) planes.

With reference to Table III, a new potential was calculated using measured discrete transitions at different particle energies. In this table a comparison is made between observed energies, and those predicted from the free-atom potential; the x-ray diffraction potential; and a new potential derived by minimizing the sum of the squares of the percent error for each transition. As seen in Figure 3, this new potential is very similar to that derived from x-ray diffraction, with a slightly higher potential midway between the chosen set of (111) planes.

Table III: Potential calcuation based upon minimization of the sum of (percent error)^2 for isolated transitions.

γ	Transition	Observed Energy	Free-Atom	Calculated energy using X-Ray Diffraction	Derived from Spectra
25.57	2 → 1	9.87	9.85 (0.0%)	9.62 (-2.6%)	9.75 (-1.2%)
25.67	3 → 0	20.6	21.90 (6.3%)	20.61 (0%)	20.58 (-0.1%)
25.67	5 → 0	28.90	31.73 (9.8%)	29.48 (2.0%)	29.28 (1.3%)
34.03	2 → 1	15.1	15.16 (0.4%)	14.93 (-1.1%)	15.17 (0.5%)
34.03	3 → 0	32.5	33.55 (3.2%)	31.75 (-2.3%)	31.69 (-2.5%)
60.76	3 → 0	72.1	76.86 (6.6%)	73.59 (2.1%)	73.37 (1.8%)
Normalized Σ(% Error)^2			7.75	1.0	0.58
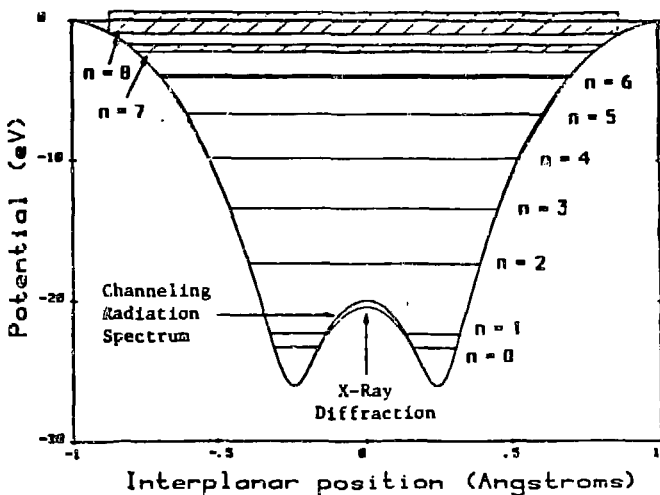
Figure 3:   The potential function derived from the channeling radiation spectrum.

The final check is to compare theory and experiment for a portion of the data not used for error minimization. This is done in Fig.4 for the data presented in Fig. 2, and it is seen that the spectrum obtained using the new function from the channeling radiation (C.R.) experiments is essentially indistinguishable from the x-ray derived calculation, and both have good agreement with the data. This result indicates that channeling radiation spectra may be used to obtain crystalline potential functions with an accuracy comparable to that using x-ray diffraction.
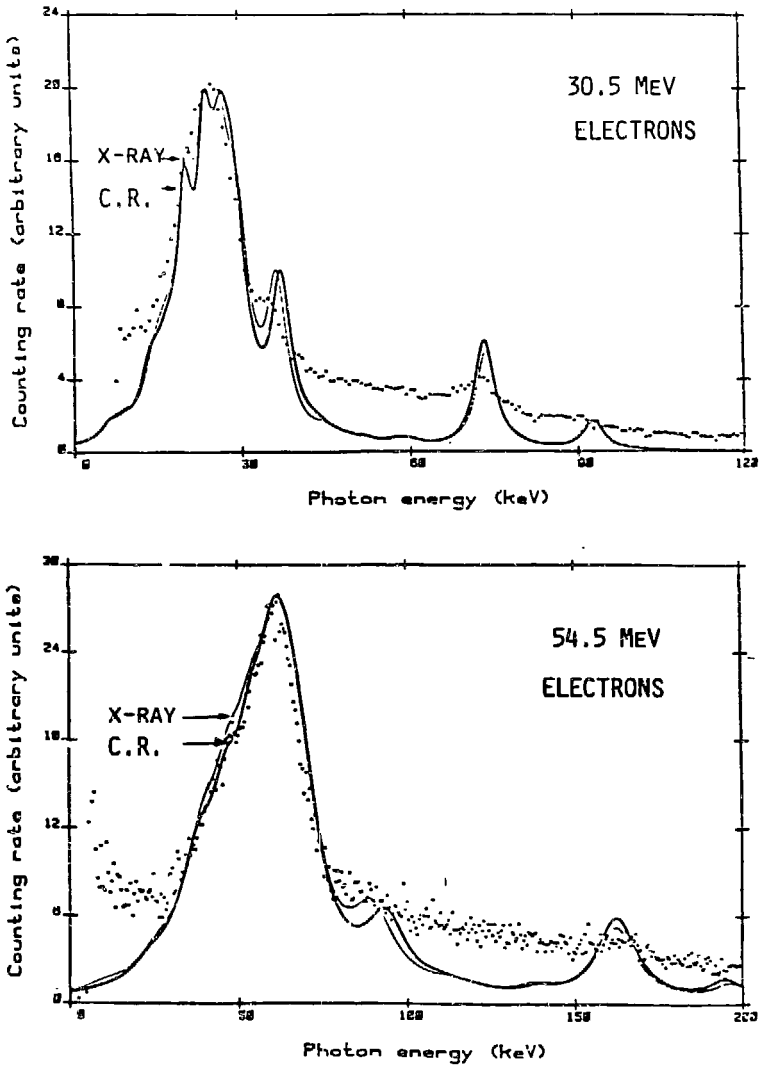

Figure 4:   Calculated continuum spectra

III. OBSERVATION OF PLATELETS IN DIAMOND

In certain types of natural diamond (Type Ia), nitrogen impurities are found in the form of atomic monolayers nucleated on (100) planes. These "platelets" distort the (100) planes, and two proposed models[4,5] for this distortion are illustrated in Fig. 5. A TEM photograph of our Type Ia diamond sample indicated platelet diameters ranging from 40 to 200 Å, with a mean separation of ~ 500Å.
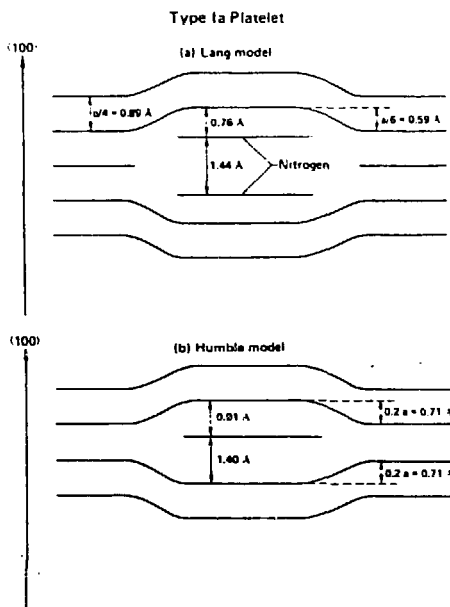

Figure 5: Distortion of (100) planes in diamond due to the presence of nitrogen platelets.

We measured electron channeling radiation from two diamond crystals, one with platelets and one without (Type IIa),[6] and the observed photon energies are listed in Table IV. Although there was a significant decrease in the intensity of the emission from (111) planes, there was essentially no change in peak photon energy. This is a reasonable result, since the platelets cause a stacking fault type of defect in (111) planes which increases scattering, but, aside from this discontinuity, the planes are undistorted. For the (100) planes, however, there are significant differences in the measured photon energies, with the calculated values closer to the measurements obtained for the crystal without platelets. In all our calculations a Debye-Waller factor is introduced to account for atomic vibrations, and for Table IV the published, rms, one-dimensional amplitude of 0.042Å was used.

Table IV: Electron channeling radiation from diamond crystals with and without nitrogen platelets.

Plane	Electron Energy		Type Ia	Photon energy (keV) Type IIa	Calculated
(111)	30.5 MeV		24.2 ± 0.6	25.0 ± 0.5	
(100)	30.5	$1 \to 0$	41.3 ± 0.4	43.0 ± 0.3	43
(100)	54.5	$1 \to 0$	111.0 ± 2	119.8 ± 0.7	122
(100)	54.4	$2 \to 1$	~ 63	64.7 ± 1.5	63

Figure 6 shows the measured radiation spectra from the two types of diamonds, for 54 MeV electrons channeled by (100) planes. The maximum emission intensity has been normalized to the same value for both curves to emphasize the difference in photon energies. To account for this frequency shift it has been assumed that the platelets introduce an uncertainty in the position of a (100) plane, as illustrated by the sketch shown in Fig. 7. The autocorrelation distance along the plane equals the platelet diameter (~ 100Å), whereas the periodic length of the wiggling motion is ~ 200Å. This suggests that an additional Debye-Waller factor might be used to describe this positional uncertainly, as illustrated by the modified potential in Fig. 8.
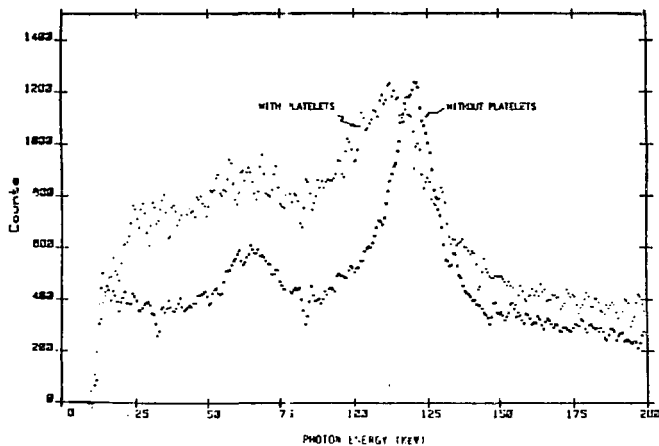

Figure 6: Radiation from 54 MeV electrons channeled along (100) planes.

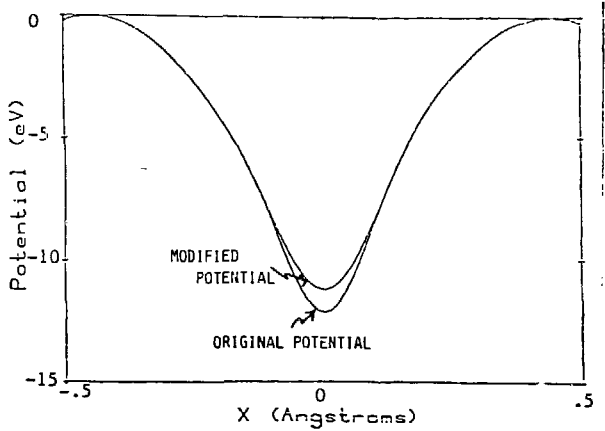Figure 7: Distortion of (100) planes due to the Platelets

Figure 8 A modified potential function to in corporate the positional
uncertainty due to platelets.

Table V contains a tabulation of measured and calculated photon energies for electrons channeled by (100) planes in a diamond with platelets. The calculated values, which are very close to the measured ones, assume a positional uncertainty of 0.038Å due to platelets, added in quadrature to the 0.042Å vibrational amplitude. A value of 0.038Å is reasonable,[7] from the models in Figure 5. This result suggests that the effects of the platelets upon the channeled particle may be represent by a Debye-Waller factor, and that the channeling radiation may be used to measure the planar distortion.

Table V: **Measured and calculated photon energies from (100) planes in a diamond crystal with platelets. The calculation uses a positional uncertainty of 0.038Å due to platelets added in quadrature to the 0.042Å vibrational amplitude.**

Particle Energy	Emission Energy for Type Ia	Calculated Emission Energy from the Modified Potential
30.5 MeV	41.3 ± 0.4 keV	41 keV
54.5	111 ± 2.0	113
54.5	~63	63

9

IV. DAMAGE EFFECTS IN LiF

Fifty-four MeV electrons were injected into three LiF crystals, close to the <100> direction, at dosages of 2.5×10^{16}, 2.5×10^{17} and 2.5×10^{18} electrons per square centimeter. Channeling radiation was then observed from 54 MeV planar-channeled electrons and positrons to determine to effects of the induced damage. Defect inducement is an important consideration for the use of channeling emission as a source of x-rays.

Figure 9 shows the channeling radiation spectra from 54 MeV electrons channeled by (110) planes in LiF. Each crystal received a different dosage of electron beam irradiation, as indicated in the figure. Each spectrum has had the random bremsstrahlung background subtracted. As the dosage increased the spectral peaks became less evident and eventually disappeared in the crystal with the highest dosage. In addition, the linewidths increased as shown in Table 8.
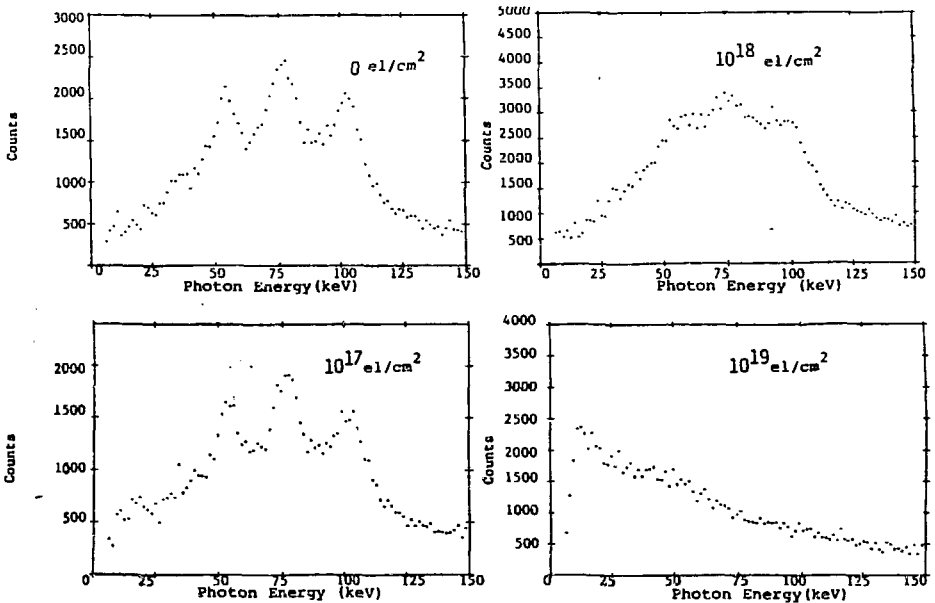

Figure 9: Channeling radiation from 54 MeV eleectron channeled by(110) planes in LiF. The crystals were subjected to defferent dosages of electron beam irradiation: 0 electrons/cm^2, 2.5×10^{16} electrons/cm^2, 2.5×10^{17} electrons/cm^2, and 2.5×10^{18} electrons/cm^2.

Table 8: Measured Linewidths for (110) Planar Channeling from 54 MeV Electrons in Damage LiF Crystals

		FWHM Measured Linewidths for Different Doses			
Transition	$h\omega$ (keV)	0 el/cm^2	2.5x10^{16}el/cm^2	2.5x10^{17}el/cm^2	2.5x10^{18}el/cm^2
1 → 0	102 keV	16.5 keV	17 keV	20.0 keV	-
2 → 1	75	14.2	15.5	17.4	-
3 → 2	54	10.3	11.6	16.1	-

The induced defects are manifested as F-centers, in which the fluorine ion is removed from its site and replaced by an electron. This results in optical absorption, so that an optical absorption spectrum may be used to determine the defect density. Using this procedure, the defect density for the 2.5x10^{17} electrons/cm^2 dosage was determined to be 1.5x10^{19} cm^{-3}. This gives a cross section σ for F-center formation of

$$\sigma = \frac{\text{defect density}}{(\text{density of F ions}) \times (\text{dosage in electrons/cm}^2)}$$

$$= 950b$$

The tabulated value[9] is 700b, which does not disagree with our measurement since our determination of dosage was not that accurate.

The cross section σ' for incoherence-inducing scattering of a channeled particle by an F-center may be calculated from the formula

$$\sigma' = \frac{1}{(l_{coh}) \times (\text{defect density})}$$

where l_{coh} is the coherence length[10] of a radiating particle. This length may be related to the full-width, half-maximum (FWHM) linewidth $\Delta\omega$ by

$$l_{coh} = \frac{\gamma^2\lambda}{\pi} \left(\frac{\omega}{\Delta\omega}\right)$$

where λ is wavelength, ω is frequency, and γ is the ratio of the channeled particle energy to its rest energy. Using the linewidths in Table 8 at a dosage of 2.5x10^{17} electrons/cm^2, the value of σ' is $\sigma' = 26\times10^{16}$cm^2. At this dosage the coherence

length due to effects other than the F-centers is relatively small, and has not been included in the calculation.

This value for σ' is extremely large, considering that the lattice constant is 4.0Å/ The result suggests that the cross section presented by an F-center is comparable to the unit cell area. preliminary results we have obtained in damaged silicon indicate that σ' is much smaller than in LiF.

Figure 10 shows the channeling radiation obtained from 54 MeV positrons, channeled by (100) planes in the same damaged crystals. It is interesting to note that whereas there is significant degradation in the electron channeling radiation at a dosage of 2.5×10^{10} electrons/cm^2, there is little change in the shape of the position emission. If one assumes the same defect density and σ' for positrons as for electrons, the effect of the damage should have been evidenced. Perhaps this means that the defects are localized near the atomic planes rather than midway between.
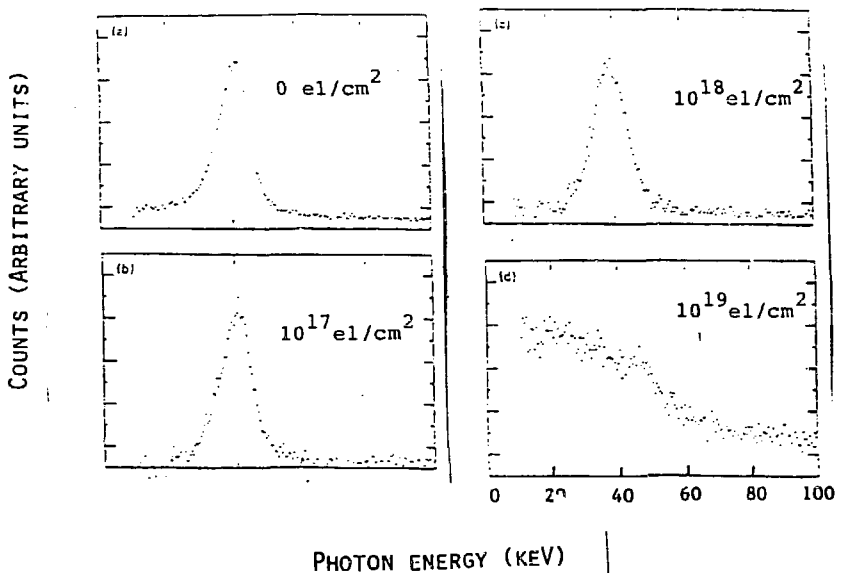

Figure 10: Channeling radiation from 54 MeV positrons, channeled by (100) planes in damage LiF crystals.

V. THERMAL VIBRATION AMPLITUDES

The vibrational motion of the atoms in a crystal affects the crystalline potential. Assuming no correlation between the motion of different atoms leads to a Debye-Waller factor[10], which reduces the depth of the potential in the vicinity of the atomic planes. This effect is shown in Figure 11, where (110) planar potentials for electrons in Si are drawn for crystal temperatures of 80 and 293K. Increasing temperature reduces the well depth and shifts the photon energy of the $1 \rightarrow 0$ transition to lower values. Photon energies for higher transitions are essentially unaffected.
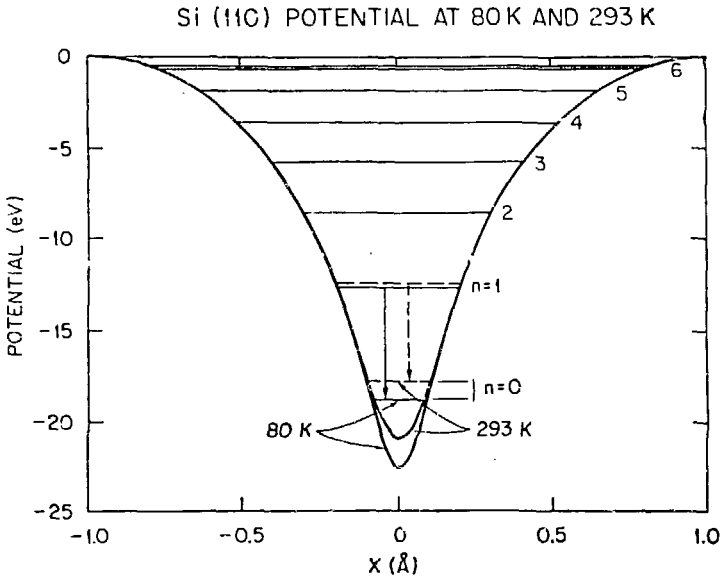
Figure 11: The electron (110) planar potential in Si at temperatures of 80 and 293K with an assumed Debye temperature of 495K. Eigenvalues are shown for 54.4 MeV electrons.

13

The observed channeling radiation spectra from 54.4 MeV electrons for two planes in Si are presented in Figure 11 for two different temperatures. As anticipated, at higher temperatures the highest peak photon energy (corresponding to the 1 → 0 transition) in the spectrum is reduced, whereas the photon energies for the other transitions are constant.
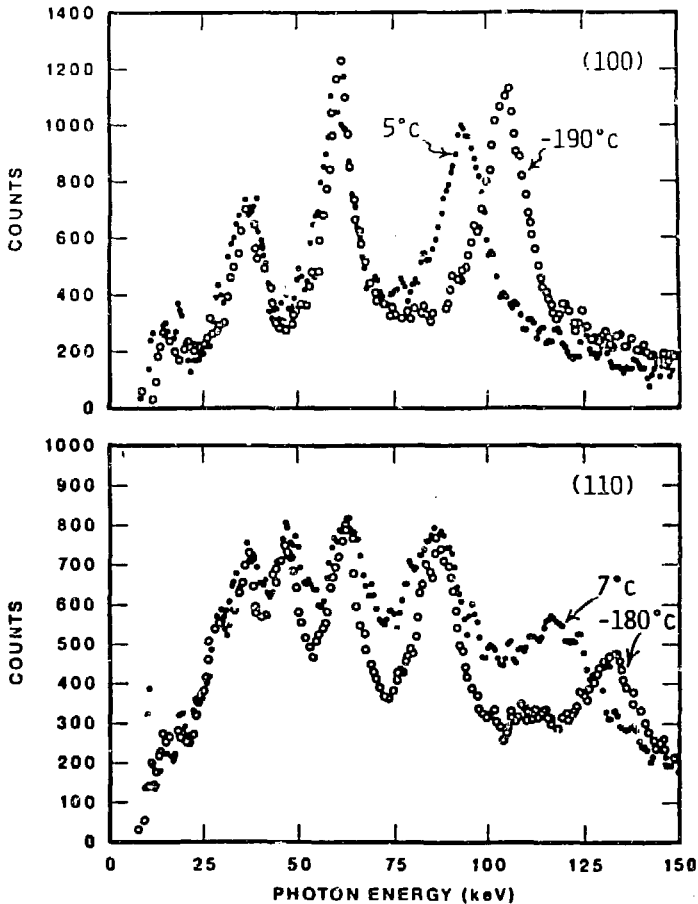

Figure 11: Radiation from 54.4 MeV electrons at different temperatures of the Si crystal. The upper figure is for (100) planes and the lower is for (110) planes.

As mentioned previously, the depth of the potential well and thus the 1 → 0 photon energy is a function of the vibrational amplitude, and so the latter can be determined from the radiation spectrum. A surrogate for vibrational amplitude is Debye temperature[11], θ_D, with a higher θ_D giving a smaller vibration.

Figure 12 shows the measured photon energies for different transitions as a function of crystal temperature, using the (110) planes in Si and 54.4 MeV electrons. The lines drawn through these data points are the calculated energies. For all transitions except $1 \to 0$, the predicted values are independent of θ_D, and the agreement between theory and experiment indicates that we have accurately determined the electron energy, and also that the potential function is valid for region not too close to the atomic planes. For the $1 \to 0$ transition the predicted photon energies agree with the data using $\theta_D = 495K$, whereas the value obtain from x-ray diffraction is $\theta_D = 549K$.
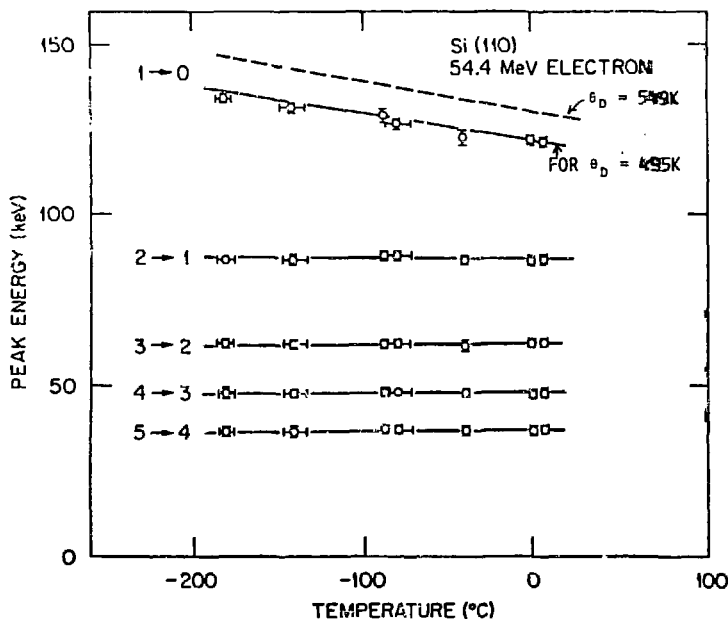

13

Figure 12: Photons energies emitted by 54.4 MeV electrons channeled by (110) planes in Si as a function of crystal temperature.

It is possible that this discrepancy results from the approximation associated with using the Debye-Waller factor to represent the effect of thermal vibrations. If this were true, one would expect similar discrepancies for other crystals, considering crystals with both higher and lower θ_D. Table 9 lists measured and calculated $1 \to 0$ photon energies using the tabulated values for θ_D, for four different crystals including Si. From this table it is seen that the largest error occurs for Si and that there is reasonably good agreement for the other three crystals. The reason for the discrepancy that exists in Si is yet to be determined.

Table 9: Measured and calculated photon energies from channeling radiation using tabulated values to Debye temperture.

Z	Crystal	Electron Energy (MeV)	θ_D(K)	u(A)	1→0 Transition Energy (keV)			
					(110) plane		(100) plane	
					Calc.	Meas.	Calc.	Meas.
6	C(Diamond)	54.4	2000	.040	163.7	161 ± 0.5	120.6	119.8 ± 0.7
14	Si	54.4	543	.075	128.5	122.2 ± 1.0	100.0	97.5 ± 1
32	Ge	16.9	290	.035	26.94	27.6 ± 0.5		
31-33	GaAs	16.9	260	.088	26.6	26.6 ± 0.4	20.5	20.6 ± 0.5

VI. CHANNELING RADIATION FROM III-V COMPOUNDS, ALLOYS AND SUPERLATTICS

We have observed planar channeling radiation, using 16.9 MeV electrons, from a GaAs crystal, from the alloy $Ga_{.7}Al_{.3}As$, and from the superlattice $Ga_{.7}Al_{.3}As/GaAs$. For the superlattice each layer is 100Å thick, the interfaces are normal to the <100> direction, and the channeling for (100) and (110) planes was performed with the direction of relativistic motion normal to the interfaces.

Figure 14 shows electron planar potentials in GaAs, $Ga_{.7}Al_{.3}As$, and $Ga_{.7}Al_{.3}As/GaAs$, for the (100), (110) and (111) planes. For the superlattice the potential was calculated by averaging the concentrations of Ga and Al over the layers, so that the potential is equivalent to the alloy $Ga_{.85}Al_{.15}As$.

Figure 15 displays the measured and calculated from (110) planes (photons per electron per steradian per keV vs photon spectra energy) for (a) GaAs, (b) $Ga_{.7}Al_{.3}As$, and (c) $Ga_{.7}Al_{.3}As/GaAs$. The sensitivity of the Ge detector decreases drastically at a photon energy of ~ 10keV, so that data below this energy is not included. Theoretical curves, shown as continuous lines, are based upon an initial 8% occupation per state (calculated for an electron beam divergence of 1.5 mrad), and using a different occupation length for each crystal to match the theory with the data. For all three cases the locations of the spectral peaks agree with the measured values. In Fig. 14a the occupation length was taken to be 5.5μ, and this gives excellent agreement between theory and experiment. In Fig. 14b the occupation length was taken to 2μ, and a length of 3μ would raise the amplitude of the theoretical curve to match the data for the peak location at 2.5 keV. Thus, the occupation length

curve to match the data for the peak location at 2.5 keV. Thus, the occupation length for the alloy is in the range from 2 to 3μ. Similarly, for the superlattice, Fig. 14c, the occupation length is from 1.7-2.4μ.   :5
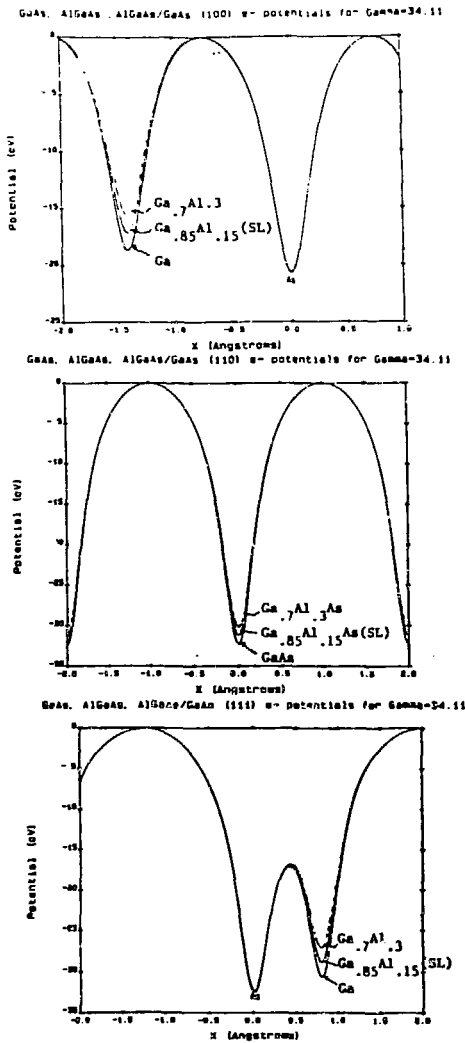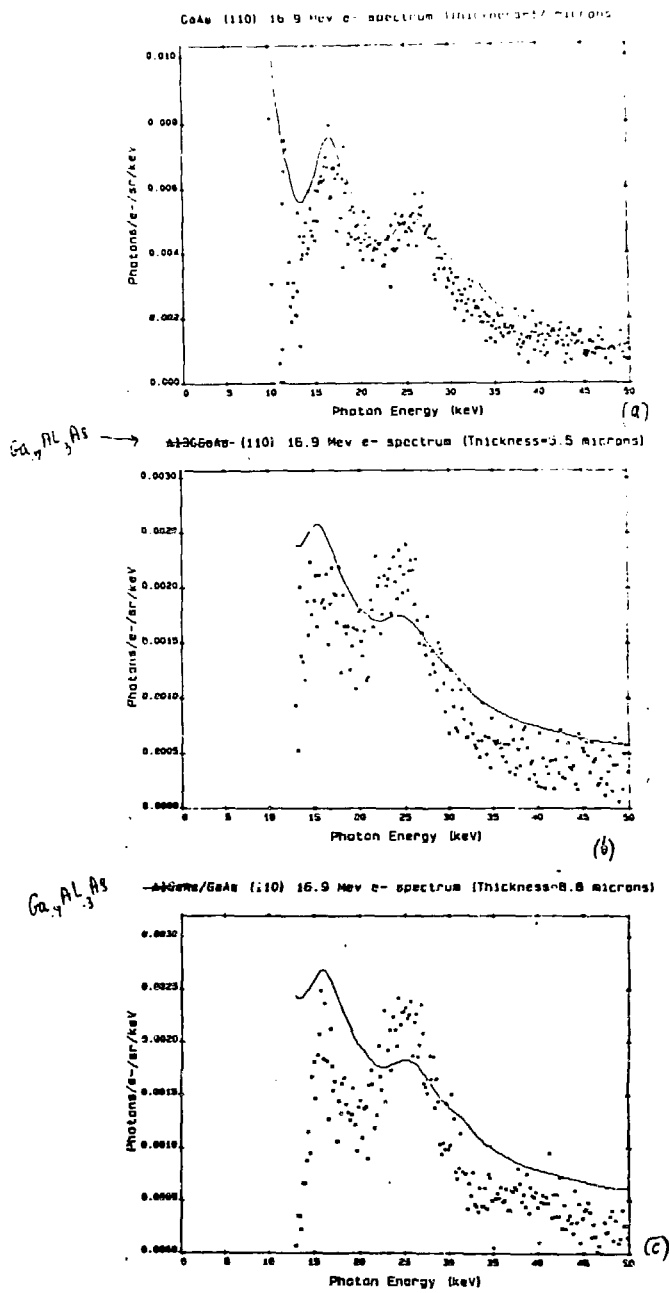
Figure 13. Electron planar potentials for GaAs, Ga$_{.7}$Al$_{.3}$As and Ga$_{.7}$Al$_{.3}$As/GaAs. Figure 13a is for (100) planes, 13b is for (110) planes, and 13c is for (111)planes.
14a   14b   14c

Figure 14: Observed and calculated spectra for 16.9 MeV electron channeling radiation from (110) planes in (a) GaAs, (b) Ga$_{.7}$Al$_{.3}$As, and (c) Ga$_{.7}$Al$_{.3}$As/GaAs.

We conclude that the occupation lengths of the channeled electrons in the alloy and superlattice are approximately one-half that in the GaAs. A calculation of the eigenstate mismatch at the interfaces of the superlattice indicates that this is not a significant dechanneling effect. Perhaps there are residual strains or defects in the alloy and superlattice that contribute to dechanneling, or perhaps the channeling is disrupted by the random introduction of Al ions.

VII. OTHER CRYSTAL TYPES AND PROPERTIES TO INVESTIGATE

An interesting crystal type to investigate by means of channeling radiation is the strained superlattice[13], (such as Si: Ge/Si) wherein the lattice constant changes from one layer to the next. Consequence of this is that the normal to a given set of crystal planes may change direction between layers, and so will add another periodicity to the motion of a channeled particle. This results in the generation of new frequencies and sidebands in the emission spectrum, which may be used to identify crystal characteristics.

Other suggested study areas include intercalated crystals[14], in which planes of carbon atoms are separated by a plane of a different atom, and ferroelectrics, wherein the crystal structure and potential change with temperature.